

Electronic Supplementary Information (ESI) for Journal of Materials Chemistry A
This journal is © The Royal Society of Chemistry 2018

Supplementary Information

Constructing channel-mediated facilitated transport membranes by incorporating covalent organic framework nanosheets with tunable microenvironments

Meidi Wang,^{ab} Fusheng Pan,^{*ab} Hao Yang,^{ab} Yu Cao,^{ab} Hongjian Wang,^{ab} Yimeng Song,^{ab} Zean Lu, Mingze Sun,^a Hong Wu,^{ab} and Zhongyi Jiang^{*ab}

^a*Key Laboratory for Green Chemical Technology of Ministry of Education, School of Chemical Engineering and Technology, Tianjin University, Tianjin 300072, China*

^b*Collaborative Innovation Center of Chemical Science and Engineering (Tianjin), Tianjin 300072, China*

* E-mail: fspan@tju.edu.cn Tel: 86-22-23500086 Fax: 86-22-23500086

* E-mail: zhyjiang@tju.edu.cn Tel: 86-22-23500086 Fax: 86-22-23500086

Section S1 Part of experimental procedures.

1.1 Synthesis of TpPa and TpBD powder

A Pyrex tube (10 mL) was charged with 63 mg of Tp (0.3mmol), 48 mg of paraphenylenediamine (0.45 mmol, for TpPa) or 82.9 mg of benzidine (0.45 mmol, for TpBD), 1.5 mL of mesitylene, 1.5 mL of dioxane and 0.5 mL of acetic acid (3 M). The mixture was next sonicated for 10 min to get a homogeneous suspension. Subsequently, the tube was sealed under vacuum after degassed by three freeze–pump–thaw cycles, and the reaction was conducted at 120 °C for 120 h. The red (TpPa) or yellow (TpBD) solid products were isolated by centrifugation and washed with anhydrous acetone, anhydrous tetrahydrofuran (THF) and anhydrous ethanol in sequence, and dried under vacuum at 120 °C for 12 h to obtain a red (TpPa) or yellow (TpBD) powder.

1.2 The detail filling amount in each hybrid membrane.

Table S1 Filler and corresponding filling amount in each hybrid membrane

Membrane	Filler	Filling amount (mg)
Pebax-Ag ⁺ @TpHz-X/PSf	Ag ⁺ @TpHz nanosheet	2, 4, 8 ,12, 16, 20
Pebax-Ag ⁺ @TpHz (Y)/PSf	Ag ⁺ @TpHz(0.5) nanosheet	3.9
	Ag ⁺ @TpHz(1.5) nanosheet	4.1
Pebax-Cu ²⁺ @TpHz/PSf	Cu ²⁺ @TpHz nanosheet	3.8
Pebax-Ni ²⁺ @TpHz/PSf	Ni ²⁺ @TpHz nanosheet	3.8
Pebax-Ag ⁺ @TpPa/PSf	Ag ⁺ @TpPa nanosheet	5.6
Pebax-Ag ⁺ @TpBD/PSf	Ag ⁺ @TpBD nanosheet	7.6

1.3 Separation experiments

The separation performance of the membranes was tested on a membrane module that was identical to reported before.¹ The thiophene/*n*-octane mixture with 500 ppm sulfur was used as feed solution, which was circulated at the rate of 40 L h⁻¹under atmospheric pressure. Meanwhile, the downstream side was under vacuum with a pressure below 0.5 kPa. After the equipment reached a steady state, the penetrants were collected in a cold trap formed by liquid nitrogen. An Agilent 6890 gas chromatograph (GC) was used to analyze the thiophene concentration of feed solution and permeate solution.

1.4 Sorption property tests

Free-standing membrane samples were firstly dried in a vacuum oven at 40 °C for 48 h. The dried membranes were weight (W_D) and immersed in thiophene/*n*-octane mixture equal for separation experiments. The immersion was carried out at 60°C and lasted for 48 h to reach sorption equilibrium. The saturated membranes were slightly wiped by filter papers and immediately weight (W_S). Subsequently the membranes were quickly transferred into a glass tube equipped with a vacuum pump. The adsorbed liquid in saturated membranes was desorbed under vacuum and collected by a cold trap. The concentration of thiophene in the adsorbed liquid was analyzed by an Agilent 6890 GC.

Section S2 Part of characterization of COFs and metal-ion@CONs.

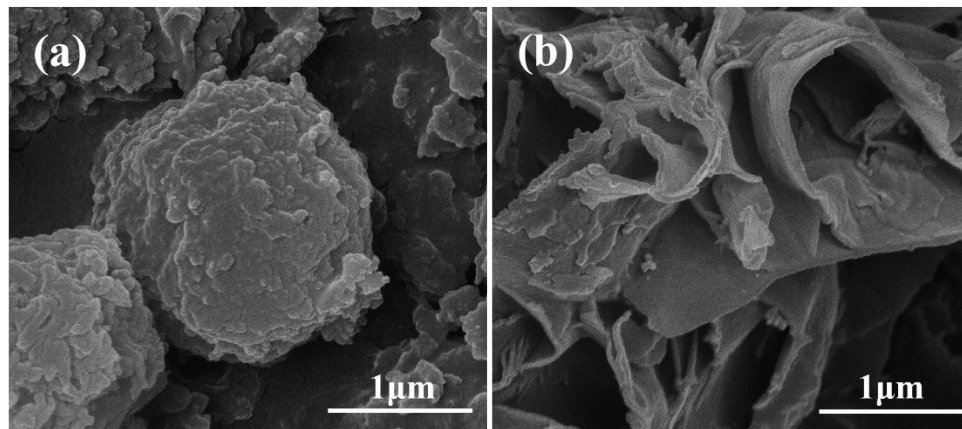


Fig. S1 SEM images of pre-exfoliated (a) TpPa and (b) TpBD.

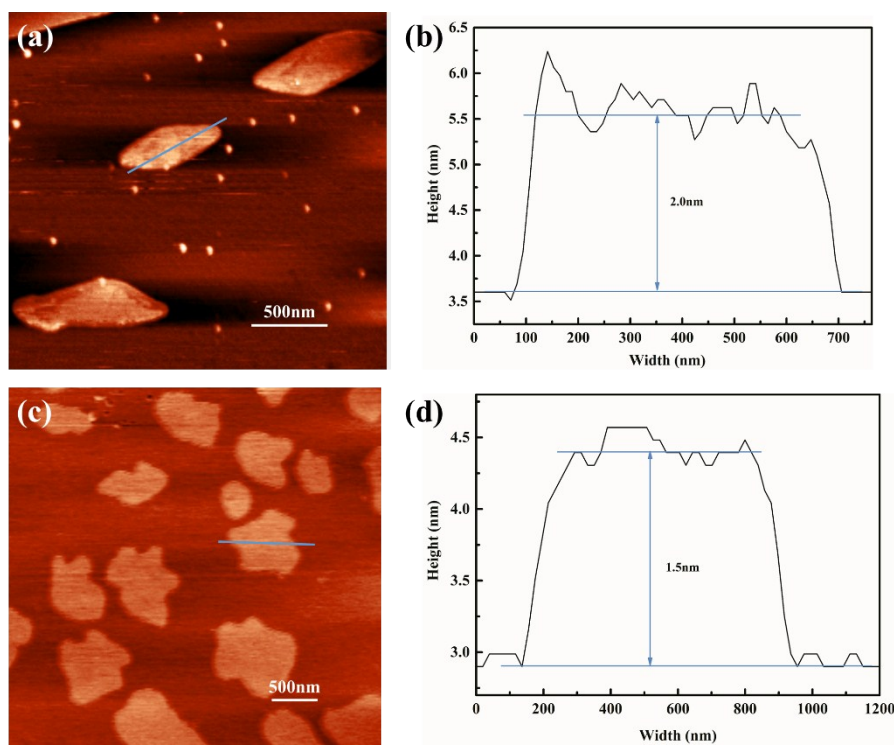


Fig. S2 AFM images of (a) $\text{Ag}^+@\text{TpPa}$ nanosheets and (c) $\text{Ag}^+@\text{TpBD}$ nanosheets, height profile of (b) $\text{Ag}^+@\text{TpPa}$ nanosheet and (d) $\text{Ag}^+@\text{TpBD}$ nanosheet.

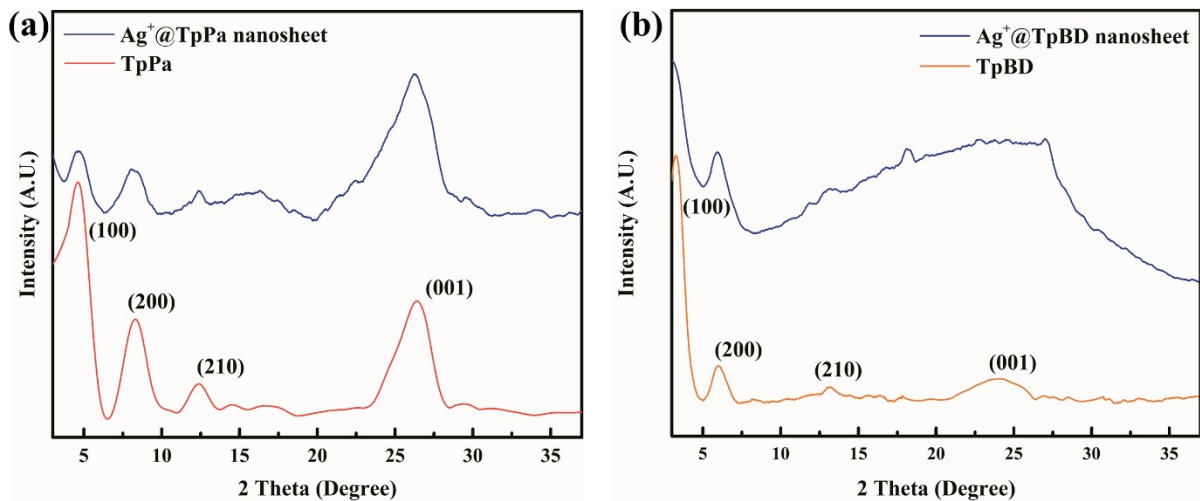


Fig. S3 XRD patterns of (a) TpPa and $\text{Ag}^+@\text{TpPa}$ nanosheet, and (b) TpBD and $\text{Ag}^+@\text{TpBD}$ nanosheet.

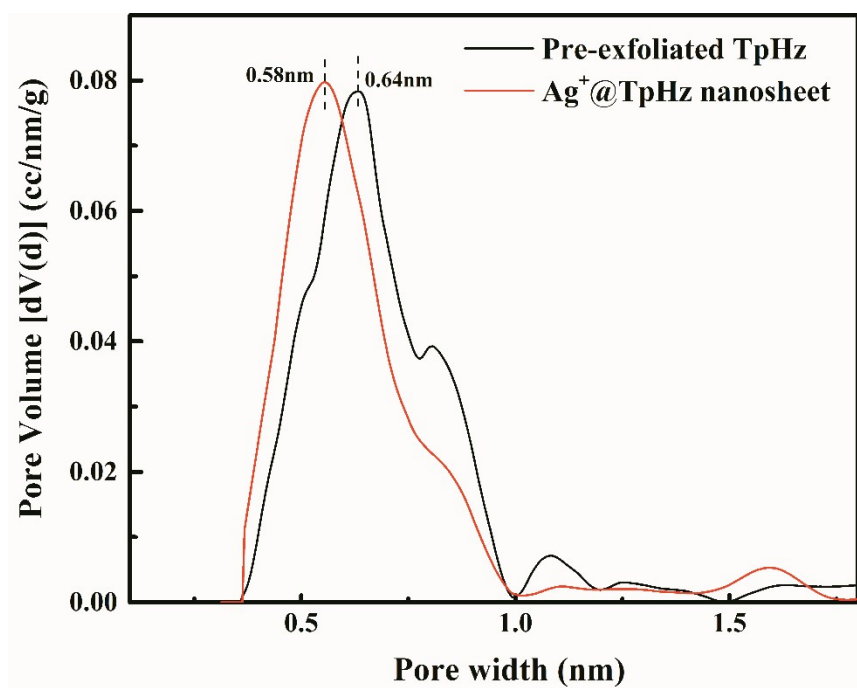


Fig. S4 Pore size distribution of pre- exfoliated TpHz (black) and $\text{Ag}^+@\text{TpHz}$ nanosheet (red).

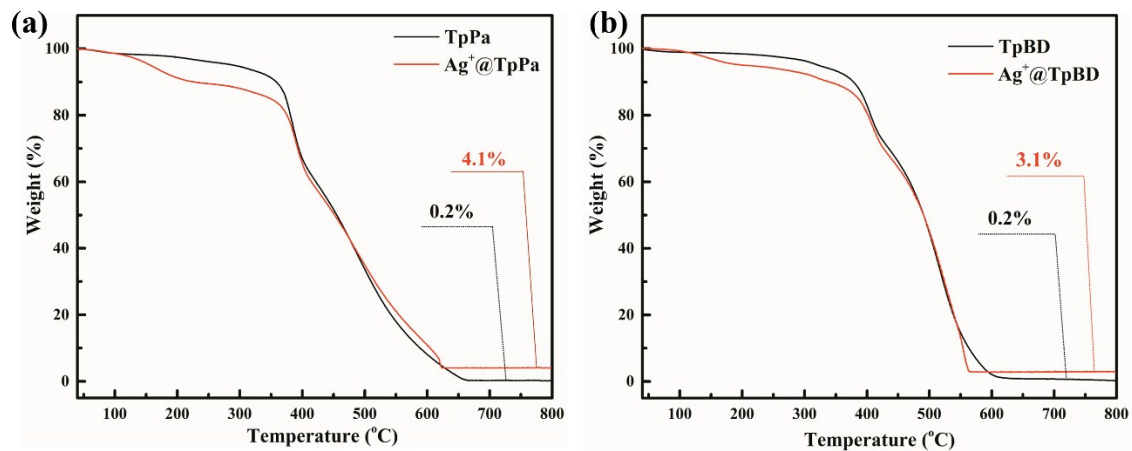


Fig. S5 Loading amount of Ag^+ on (a) $\text{Ag}^+@\text{TpPa}$ nanosheets and (b) $\text{Ag}^+@\text{TpBD}$ nanosheets.

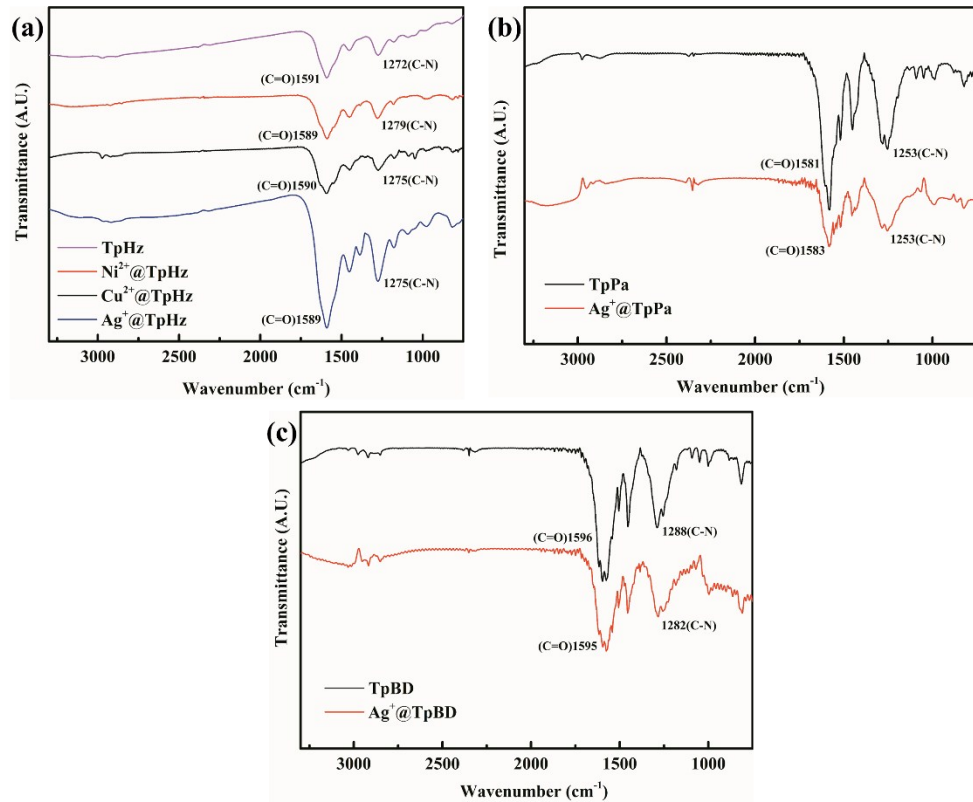


Fig. S6 FTIR spectra of (a) TpHz and metal-ion@TpHz nanosheets, (b) TpPa and $\text{Ag}^+@\text{TpPa}$ nanosheets, (c) TpBD and $\text{Ag}^+@\text{TpBD}$ nanosheets.

Section S3 Part of characterization of membranes.

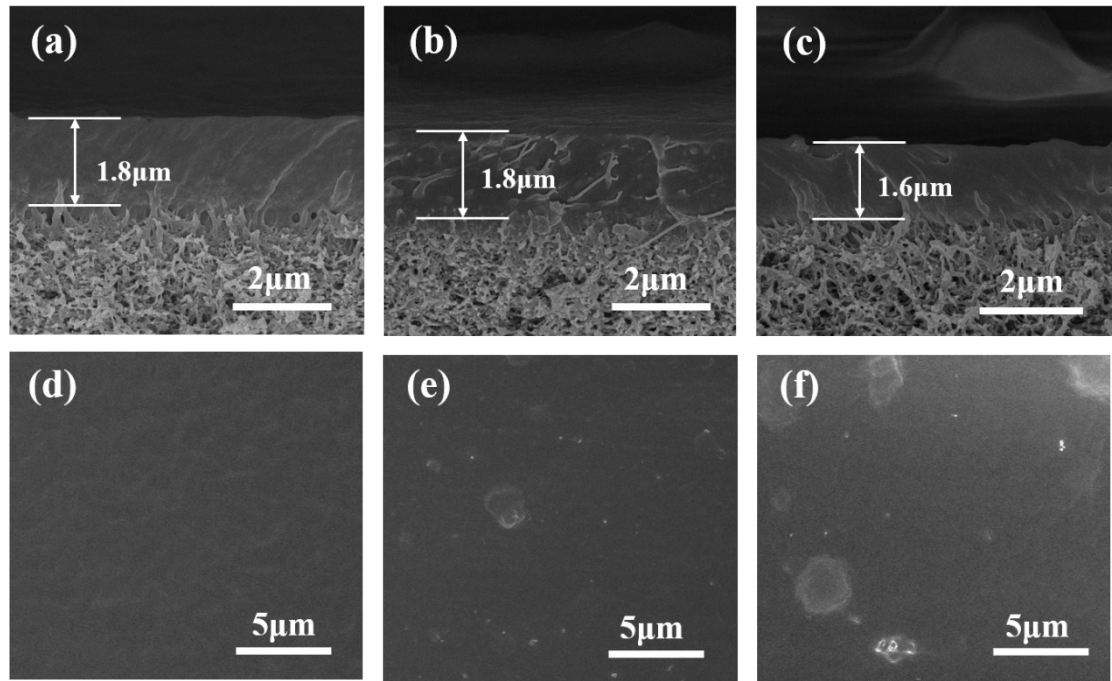


Fig. S7 SEM cross-sectional images of (a) Pebax/PSf, (b) Pebax-Ag⁺@TpHz-0.8/PSf, (c) Pebax-Ag⁺@TpHz-2.0/PSf ; SEM surface images of (d) Pebax/PSf, (e) Pebax-Ag⁺@TpHz-0.8/PSf, (f) Pebax-Ag⁺@TpHz-2.0/PSf.

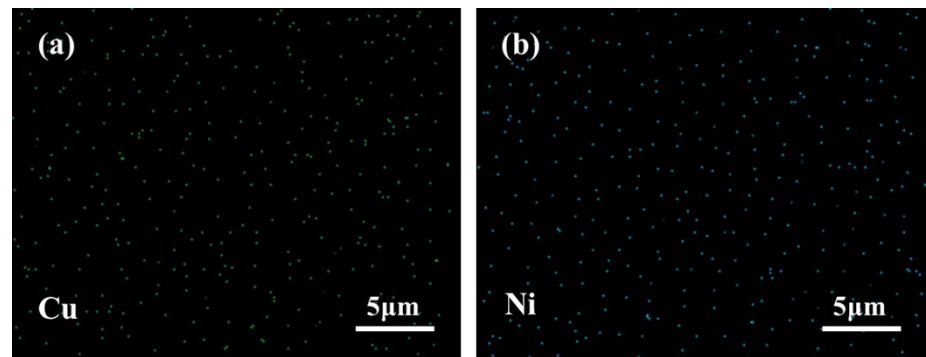


Fig. S8 Elemental mapping for (a) Cu in Pebax-Cu²⁺@TpHz/PSf and (b) Ni in Pebax-Ni²⁺@TpHz/PSf.

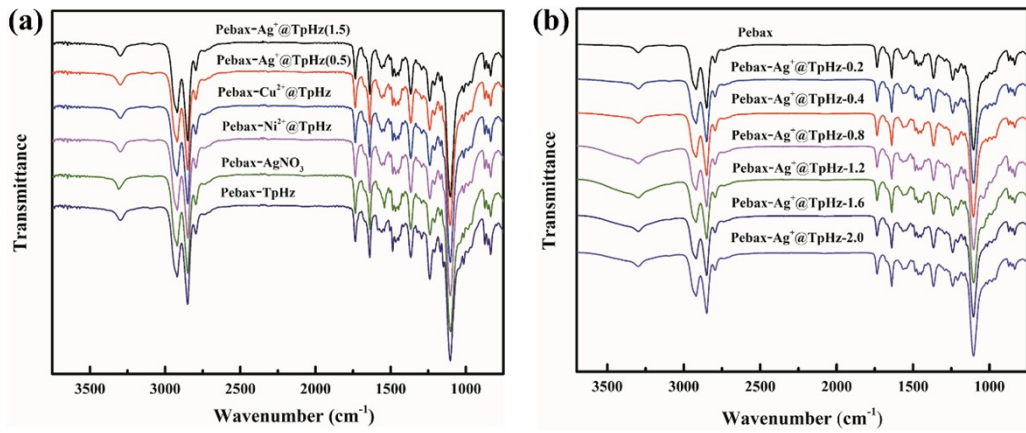


Fig. S9 FTIR spectra of (a) Pebax and Pebax-Ag⁺@TpHz-X/PSf and (b) some facilitated transport membranes in this research.

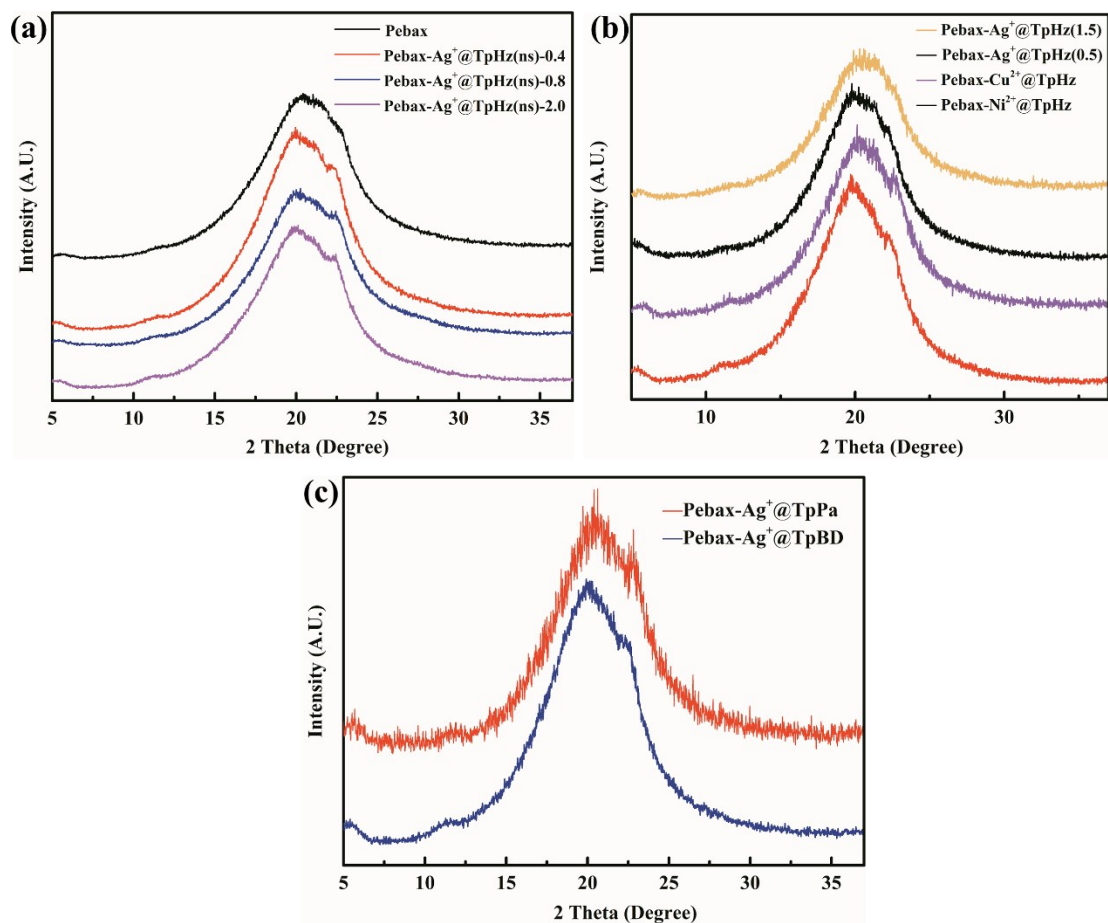


Fig. S10 XRD patterns of (a) Pebax and Pebax-Ag⁺@TpHz-X membranes, (b) the membranes separately incorporating different metal-ion@TpHz nanosheets and (c) the membranes separately incorporating different metal-ion@TpPa and TpBD.

$\text{Ag}^+@\text{CONs}$.

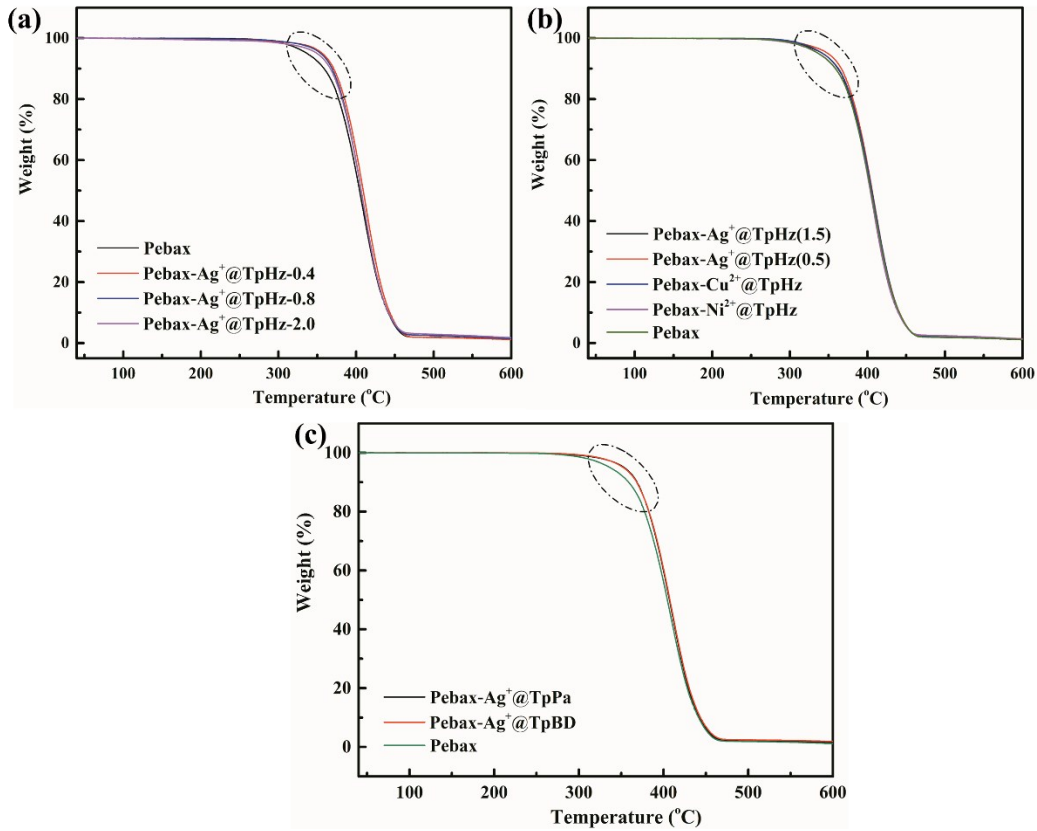


Fig. S11 TGA curves of (a) Pebax and Pebax-Ag⁺@TpHz-X membranes, (b) the membranes separately incorporating different metal-ion@TpHz nanosheets and (c) the membranes separately incorporating different

$\text{Ag}^+@\text{CONs}$.

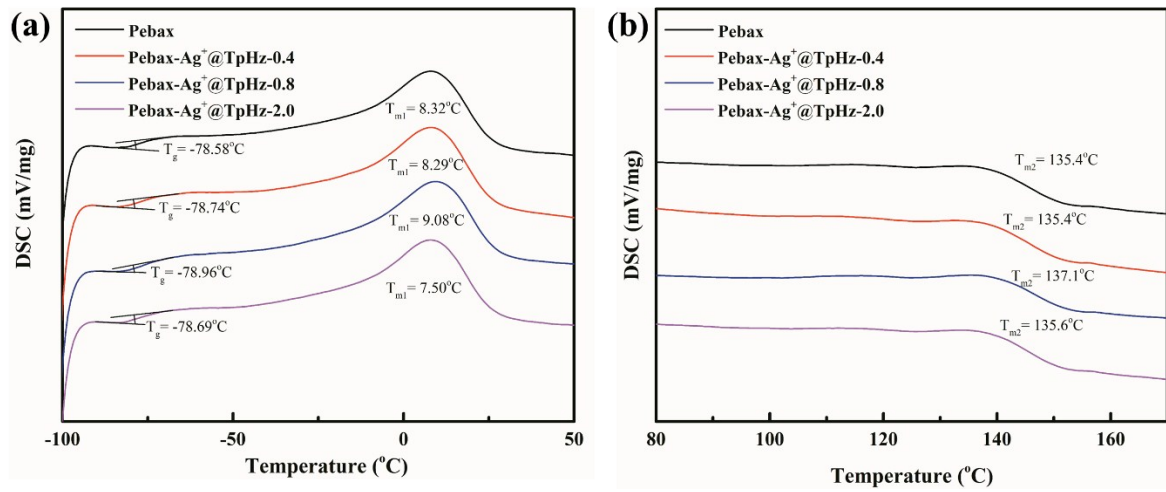


Fig. S12 DSC curves of the pristine Pebax membrane and Pebax-Ag⁺@TpHz- X , (a) low temperature zone and (b)

high temperature zone.

Section S4 Part of separation performance of facilitated transport membranes.

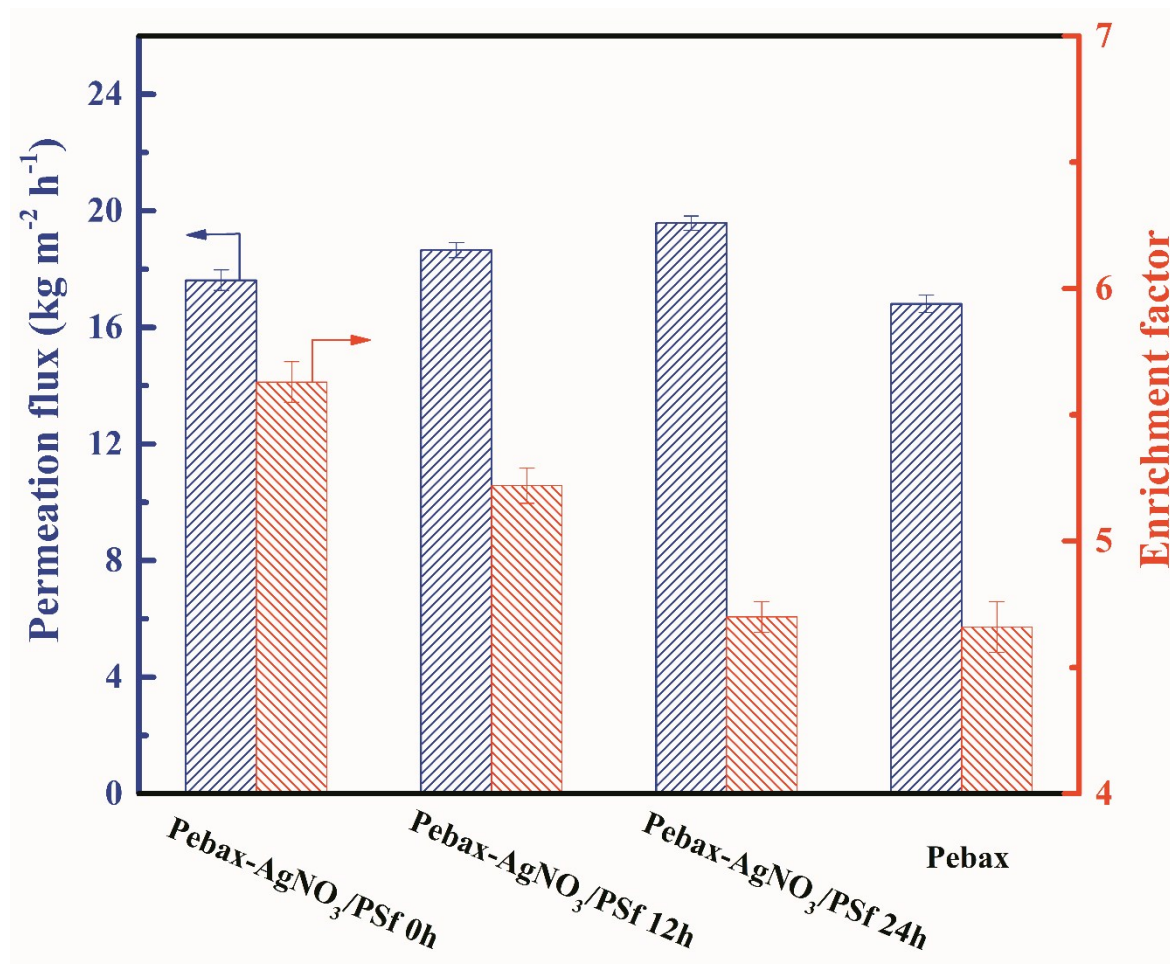


Fig. S13 The stability test of Pebax- AgNO_3/PSf .

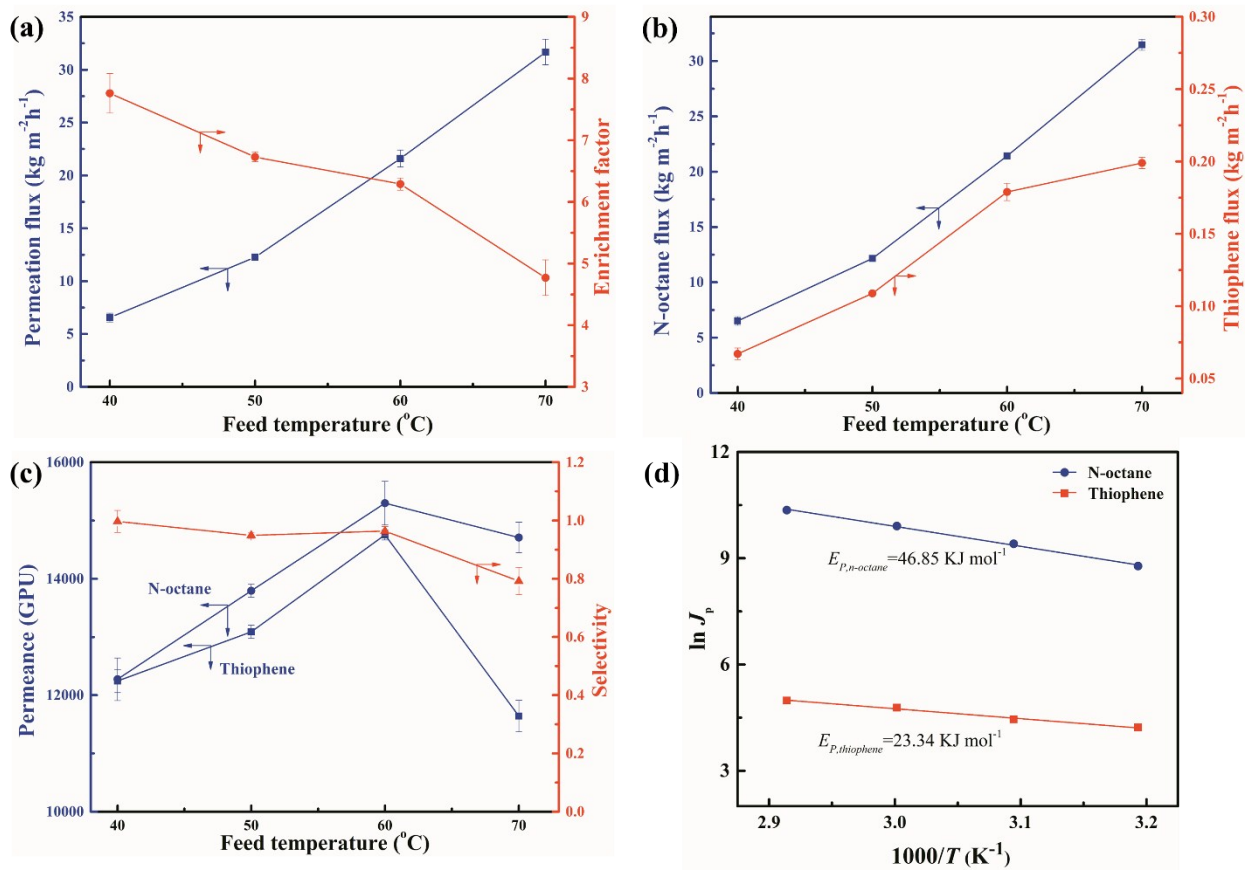


Fig. S14 Effect of operation temperature on (a) total flux and enrichment factor, (b) *n*-octane flux and thiophene flux, and (c) permeance and selectivity of Pebax-Ag⁺@TpHz-0.4/PSf for the desulfurization of 1312 ppm *n*-octane/thiophene mixtures, and (d) Arrhenius plots of *n*-octane and thiophene fluxes.

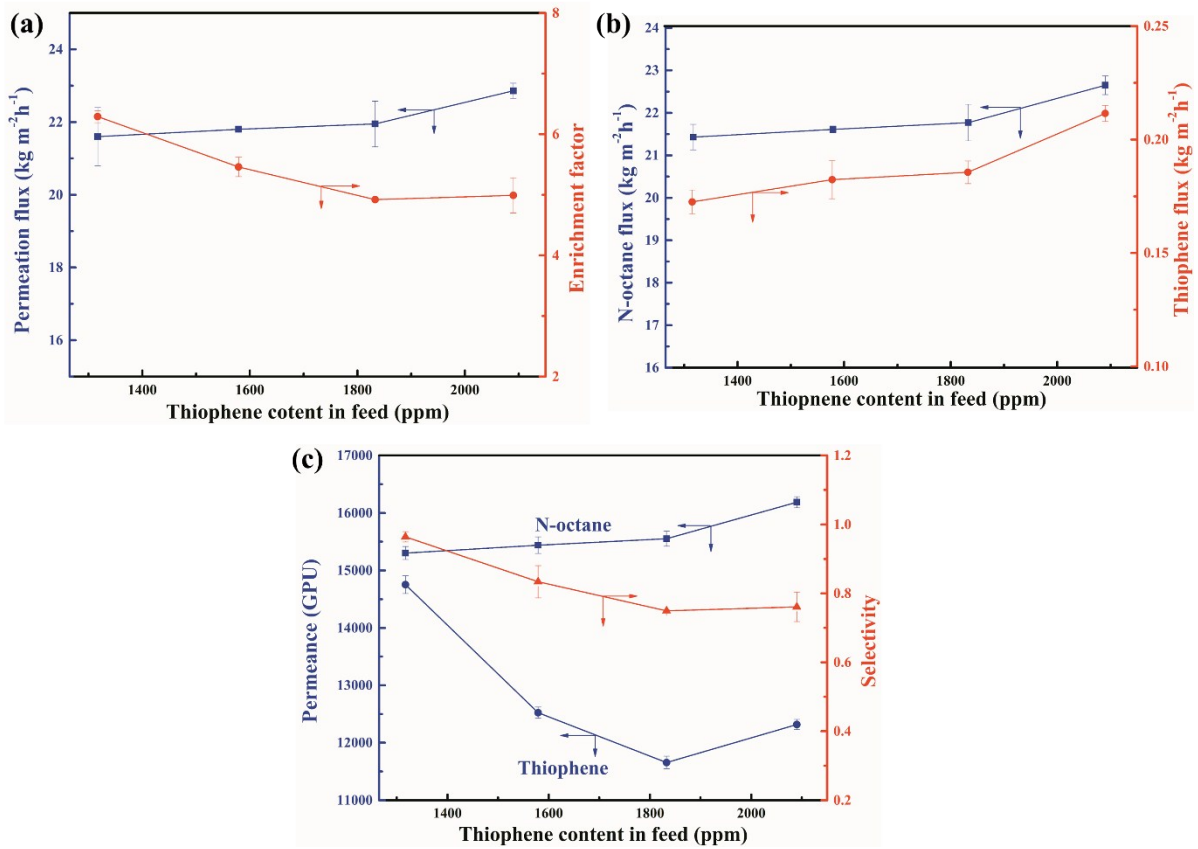


Fig. S15 Effect of thiophene concentration in feed solution on the (a) total flux and enrichment factor, (b) thiophene flux and *n*-octane flux, and (c) permeance and selectivity of Pebax-Ag⁺@TpHz-0.4/PSf for the desulfurization of *n*-octane/thiophene mixtures on 60°C.

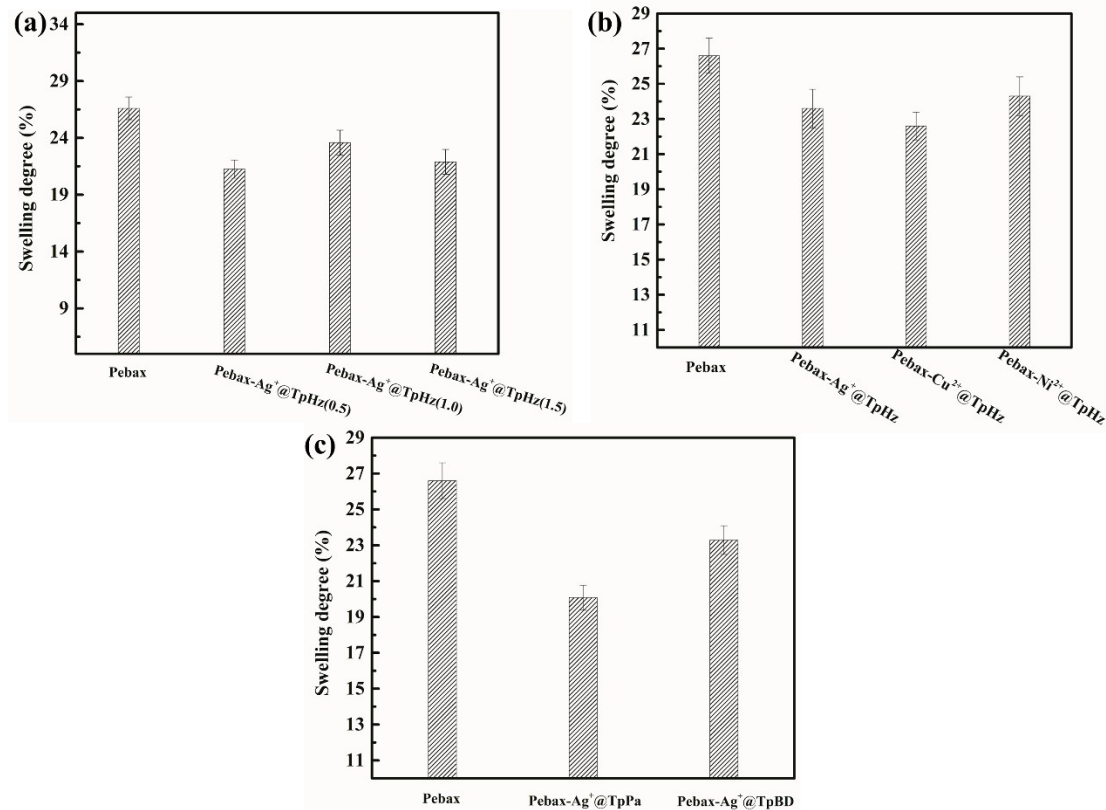


Fig. S16 Swelling degree of (a) the pristine Pebax membrane and membranes separately incorporating different $\text{Ag}^+@\text{TpHz}$ nanosheets, (b) the pristine Pebax membrane and membranes separately incorporating different metal-ion@TpHz nanosheets, (c) the pristine Pebax membrane and membranes separately incorporating different $\text{Ag}^+@\text{CONs}$.

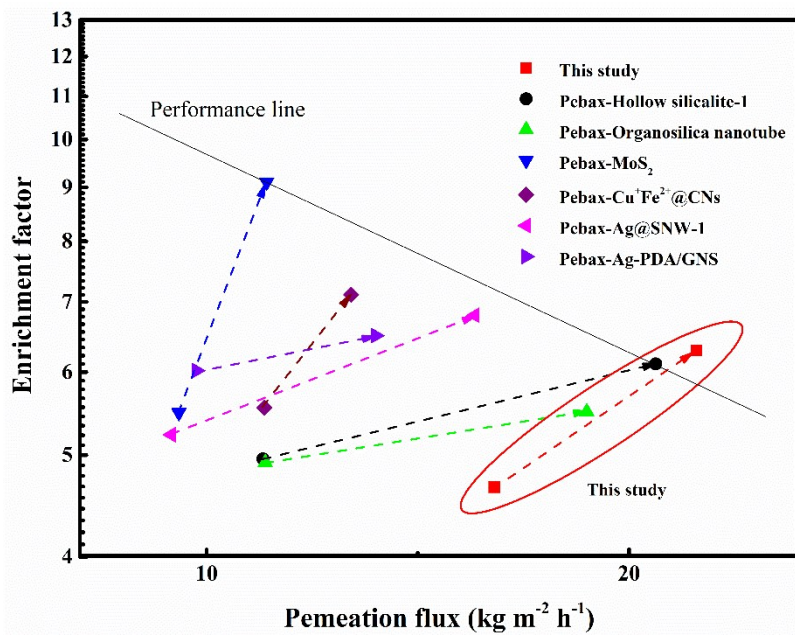


Fig. S17 Illustration of performance improvement of typical pristine Pebax membranes.

Section S5 Comparison of separation performance with other desulfurization membranes.

Table S2 Comparison of the membrane separation performance in this study with previous desulfurization membranes in literatures.

Membrane	Temperature (K)	Sulfur content in feed (ppm)		Thickness (μm)	Pervaporation performance			Reference
		Permeation flux (kg m ⁻² h ⁻¹)	Enrichment factor		Thiophene permeability (GPU)	Selectivity		
Pebax-Ag ⁺ @TpHz-0.4/PSf	333	500	1.8	21.6	6.29	14753	0.964	This work
Pebax-Ag ⁺ @TpHz-0.8/PSf	333	500	1.8	22.44	6.04	/	/	This work
Pebax-MoS ₂ -4/PSf	333	500	1.8	11.42	9.11	8050	1.4	2
Pebax-HPSiNT(2)/PSf	333	500	1.8	19	5.5	11400	0.85	3
Pebax-CuBTC(2%)	333	500	2	12	4.4	/	/	4
Peabx-HMS(200)-20/PSf	333	500	1.8	20.63	6.11	13800	0.93	5
PDMS-Cu@UiO-67b	313	500	10	8.1	4.2	/	/	6
Pebax-Ag ⁺ @SNW-1-9/PSf	333	500	2	16.35	6.80	12099	1.046	7
Pebax-Cu ⁺ Fe ²⁺ @CNs-5/PSf	333	500	2	13.42	7.11	10399	1.095	8
PDMS-MIL101(Cr)-6/PVDF	313	500	15	5.2	5.6	6857	0.703	9
PDMS-NH3-(TMOS)16/PSf	303	500	/	7.36	4.98	13373	0.543	10
Pebax/PVDF	313	1280	11	3.8	4.0	3527	0.496	11
PDMS-dopamine/Cu/PSf	303	500	16	7.42	4.81	8340	0.598	12
PDMS-DATi(2.2.2.2)/PSf	313	500	18	6.61	4.80	7413	0.597	13
Ethyl Cellulose-C60	348	300	/	2.32	4.72	844	0.781	14
PEG	358	300	/	0.58	9.39	432	1.606	15
PDMS	393	566	/	0.64	4.83	261	0.880	16
PEG-CuY	383	1190	/	3.19	2.95	780	0.527	17
PDMS-DAAg/5-5.0/PSf	313	500	16~25	8.22	5.03	9682	0.627	18
PDMS-Ag ⁺ /TiO ₂ (0.01)-5.0/PSf	313	500	/	4.14	8.56	8590	1.110	19

PDMS-GNS(0.2)/PVDF	313	500	20	6.22	3.58	5143	0.439	20
PDMS-CuBTC-8/PVDF	313	500	35	6.47	5.20	7891	0.649	21
PDMS-Ni ²⁺ Y/PSf	303	500	>50	3.26	4.84	/	/	22
PDMS-AgY/PAN	323	/	15	8.15	3.45	4428	0.481	23
PEG/PU	383	1200	/	2.5	4.03	838	0.725	24
PEG/PES	378	238	15.5	3.37	3.63	/	/	25
Cl-PBPP	353	400	12.4	1.38	5.6	605	0.944	26
Pebax-Ag-PDA/GNS-6/PSf	313	500	6	4.42	8.76	9404	1.139	27
Pebax-Ag-PDA/GNS-6/PSf	333	500	6	14	6.48	9859	0.995	27

Table S3 The performance of the pristine Pebax membranes and the corresponding hybrid membranes.

Filler	Permeation flux of pristine membrane /($\text{kg m}^{-2} \text{ h}^{-1}$)	Enrichment factor of pristine Pebax membrane	Permeation flux of hybrid membrane /($\text{kg m}^{-2} \text{ h}^{-1}$)	Enrichment factor of hybrid membrane	The increase percentage of permeation flux /%	The increase percentage of enrichment factor /%	Removal rate of thiophene*/($\text{kg m}^{-2} \text{ h}^{-1}$)	Reference
$\text{Ag}^+@\text{TpHz}$	16.81	4.66	21.60	6.29	29	35	0.178	This study
Hollow silicalite-1	11.33	4.96	20.63	6.11	82	23	0.165	5
Pebax-CuBTC (2%)	<12	<4.4	12	4.4	/	/	0.069	4
Organosilica nanotubes	11.39	4.92	19.0	5.5	66	11	0.137	3
MoS_2	9.34	5.49	11.42	9.11	22	65	0.136	2

Cu ⁺ Fe ²⁺ @CNs	11.37	5.55	13.42	7.11	18	28	0.125	8
Ag ⁺ @SNW-1	9.16	5.23	16.35	6.8	78	30	0.145	7
Ag-PDA/GNS	8.76	6.02	14	6.5	64	8	0.119	27

*The removal rate of thiophene is obtained by the equation: $E = J \times \beta \times \omega^F$

References

1. W.P. Liu, Y.F. Li, X.X. Meng, G.H. Liu, S. Hu, F.S. Pan, H. Wu, Z.Y. Jiang, B.Y. Wang, Z.X. Li, X.Z. Cao, *J. Mater. Chem. A*, 2013, **1**, 3713-3723.
2. F.S. Pan, H. Ding, W.D. Li, Y.M. Song, H. Yang, H. Hong, Z.Y. Jiang, B.Y. Wang, X.Z. Cao, *J. Membr. Sci.*, 2018, **545**, 29-37.
3. F.S. Pan, H.J. Wang, W.D. Li, S.B. Zhang, J. Sun, H. Yang, M.D. Wang, M.R. Wang, X.D. Zhou, X. Liu, Z.Y. Jiang, *Chem. Eng. Sci.*, 2019, **195**, 609-618.
4. S.N. Yu, Z.Y. Jiang, W.D. Li, J.Q. Mayta, H. Ding, Y.M. Song, Z. Li, Z. W. Zhi, F.S. Pan, B.Y. Wang, P. Zhang, X.Z. Cao, *Chem. Eng. Process.*, 2018, **123**, 12-19.
5. F.S. Pan, W.D. Li, Y. Zhang, J. Sun, M.D. Wang, H. Wu, Z.Y. Jiang, L.G. Lin, B.Y. Wang, X. Z. Cao, P. Zhang, *AIChE J.*, 2019, **65**, 196-206.
6. Y. M. Song, H. Ding, S. Yang, S.N. Yu, X. S. Teng, Z. Chang, F. S. Pan, X. H. Bu, Z. Y. Jiang, B. Y. Wang, S. Wang and X. Z. Cao, *Sep. Purif. Technol.*, 2019, **210**, 258-267.
7. F.S. Pan, M. Wang, H. Ding, Y. Song, W. Li, H. Wu, Z. Jiang, B. Wang, X. Cao, *J. Membr. Sci.*, 2018, **552**, 1-12.
8. H. Ding, F.S. Pan, E. Mulalic, H. Gomaa, W.D. Li, H. Yang, H. Wu, Z.Y. Jiang, B.Y. Wang, X.Z. Cao, P. Zhang, *J. Membr. Sci.*, 2017, **526**, 94-105.
9. S.N. Yu, F.S. Pan, S. Yang, H. Ding, Z.Y. Jiang, B.Y. Wang, Z.X. Li, X.Z. Cao, *Chem. Eng. Sci.*, 2015, **135**, 479-488.
10. B. Li, W.P. Liu, H. Wu, S.N. Yu, R.J. Cao, Z.Y. Jiang, *J. Membr. Sci.*, 2012, **415**, 278-287.
11. K. Liu, C.J. Fang, Z.Q. Li, M. Young, *J. Membr. Sci.*, 2014, **451**, 24-31.
12. W.P. Liu, Y.F. Li, X.X. Meng, G.H. Liu, S. Hu, F.S. Pan, H. Wu, Z.Y. Jiang, B.Y. Wang, Z.X. Li, X.Z. Cao, *J. Mater. Chem. A*, 2013, **1**, 3713-3723.
13. W.P. Liu, S. Hu, G.H. Liu, F.S. Pan, H. Wu, Z.Y. Jiang, B.Y. Wang, Z.X. Li, X.Z. Cao, *J. Mater. Chem. A*, 2014, **2**, 5267-5279.
14. S. Sha, Y. Kong, J.R. Yang, *Energy Fuels*, 2012, **26**, 6925-6929.
15. L.G. Lin, Y. Kong, G. Wang, H.M. Qu, E.R. Yang, D.Q. Shi, *J. Membr. Sci.*, 2006, **285**, 144-151.
16. L.G. Lin, G. Wang, H.M. Qu, J.R. Yang, Y.F. Wang, D.Q. Shi, Y. Kong, *J. Membr. Sci.*, 2006, **280**, 651-658.
17. L.G. Lin, Y.H. Zhang, H. Li, *J. Colloid Interface Sci.*, 2010, **350**, 355-360.
18. G.H. Liu, T.T. Zhou, W.P. Liu, S. Hu, F.S. Pan, H. Wu, Z.Y. Jiang, B.Y. Wang, J. Yang, X.Z. Cao, *J. Mater. Chem. A*, 2014, **2**, 12907-12917.
19. W.P. Liu, B. Li, R.J. Cao, Z.Y. Jiang, S.N. Yu, G.H. Liu, H. Wu, *J. Membr. Sci.*, 2011, **378**, 382-392.
20. D. Yang, S. Yang, Z.Y. Jiang, S.N. Yu, J.L. Zhang, F.S. Pan, X.Z. Cao, B.Y. Wang, *J. J. Membr. Sci.*, 2015, **487**, 152-161.
21. S.N. Yu, Z.Y. Jiang, H. Ding, F.S. Pan, B.Y. Wang, J. Yang, X.Z. Cao, *J. Membr. Sci.*, 2015, **481**, 73-81.
22. B. Li, D. Xu, Z.Y. Jiang, X.F. Zhang, W.P. Liu, D. Xiao, *J. Membr. Sci.*, 2008, **322**, 293-301
23. R.B. Qi, Y.J. Wang, J. Chen, J.D. Li, S.L. Zhu, *J. Membr. Sci.*, 2007, **295**, 114-120.
24. L.G. Lin, Y. Kong, K.K. Xie, F.W. Lu, R.K. Liu, L. Guo, S. Shao, J.R. Yang, D.Q. Shi, Y.Z. Zhang, *Sep. Purif. Technol.*, 2008, **61**, 293-300.

25. Y. Kong, L.G. Lin, Y.Z. Zhang, F. W. Lu, K.K. Xie, R. K. Liu, L. Gou, S. Shao, J.R. Yang, D. Q. Shi, *Eur. Polym. J.*, 2008, **44**, 3335-3343.
26. Z.J. Yang, Z.Q. Wang, J. Li, J.X. Chen, *Sep. Purif. Technol.*, 2013, **109**, 48-54.
27. S.N. Yu, Z.Y. Jiang, S. Yang, H. Ding, B.F. Zhou, K. Gu, D. Yang, F.S. Pan, B.Y. Wang, S. Wang, X.Z. Cao, *J. Membr. Sci.*, 2016, **514**, 440-449